

Numerical Analysis of Flow around Rectangular Cylinders with Various Side Ratios

Akira Rokugou¹, Atsushi Okajima², Kohji Kamiyama³

1. YKK Corp., 200 Yoshida, Kurobe, Toyama, Japan, E-mail:rrokugou@rd.ykk.co.jp

2. Dept. of Mech. Eng., Kanazawa Univ., 2-40-20 Kodatsuno, Kanazawa, Ishikawa, Japan,
E-mail:okajima@t.kanazawa-u.ac.jp

3. Graduate School, Tokyo Inst. of Tech., 2-12-1 Ookayama, Meguro, Tokyo, Japan,
E-mail:kamiyama@stu.mech.timech.ac.jp

Corresponding author Akira Rokugou

Abstract

Three-dimensional numerical analysis of the flow around rectangular cylinders with various side ratios, D/H, from 0.2 to 2.0, was carried out for Reynolds number of 1000 by using a multi directional finite difference method on a regular-arranged multi grid. The predicted results are in good agreement with the experimental data. It is found that fluid dynamic characteristics of rectangular cylinders alternate between the high-pressure mode and the low-pressure mode of the base pressure for D/H=0.2-0.6. We show that this phenomenon is induced by the change of the flow pattern around rectangular cylinders.

Keyword: Separated Flow, Wake, Vortex, Fluid Force, Rectangular Cylinder

1. Introduction

The flow around a circular or rectangular cylinder in the uniform flow is the most basic fluid dynamic phenomenon. It is known that the flow around a rectangular cylinder exhibits an unsteady behavior such as full-separation flow, alternately reattachment flow and full-reattachment flow, accompanied by a change in fluid dynamic force according to changes in its side ratio, D/H, where D is the flow-direction length and H is the cross-flow direction length of a rectangular cylinder, and Reynolds number. In particular in high Reynolds number, Nakaguchi et al.⁽¹⁾ found by the wind tunnel experiment that drag coefficient and base pressure coefficient had peak values in a D/H=0.6 cylinder which has a flat cross flow section. Although, as in the work of Bearman et al.⁽²⁾, many studies were carried out to resolve the above mentioned phenomenon, using high Reynolds number of approximately $Re=10^4$. Recently, a fluid tunnel experiment in comparatively low Reynolds number region, $Re=(0.67-6.7) \times 10^4$, was carried out by Ohya⁽³⁾ and he found that the flow pattern around a rectangular cylinder with a side ratio D/H=0.5 was temporally and irregularly changed between the high-pressure mode and low-pressure mode of base pressure coefficient. Okajima et al.⁽⁴⁾ carried out an experiment using low Reynolds number, $Re=10^3$, and found that the change in base pressure coefficient was dependent on Reynolds number by the wind tunnel studies. On the other hand, some numerical studies were recently carried out to resolve this phenomenon. Enya et al.⁽⁵⁾ calculated the flow around rectangular cylinders with side ratios D/H=0.2-1.0 in high Reynolds number using the LES model. In this study, they simulated the same phenomenon in the experimental study of Ohya, and clarified the relationship between flow pattern and base pressure coefficient. Hayashi and Ohya.⁽⁶⁾⁽⁷⁾ calculated the flow around rectangular cylinders with side ratios, D/H=0.4-0.6, in low Reynolds number, $Re=(1.0-3.0) \times 10^3$, by the large-scale DNS with over 13 million mesh points, and found the same phenomenon occurring in low Reynolds number.

In this study, numerical analysis of a three-dimensional flow field around rectangular cylinders with side ratios D/H=0.2-2.0, which involves D/H=0.6, the critical depth in high Reynolds number, in comparatively low Reynolds number, $Re=10^3$, has been carried out. Then the changes of fluid dynamic characteristics with the side ratios in low Reynolds number have been compared with

Report Documentation Page			Form Approved OMB No. 0704-0188	
<p>Public reporting burden for the collection of information is estimated to average 1 hour per response, including the time for reviewing instructions, searching existing data sources, gathering and maintaining the data needed, and completing and reviewing the collection of information. Send comments regarding this burden estimate or any other aspect of this collection of information, including suggestions for reducing this burden, to Washington Headquarters Services, Directorate for Information Operations and Reports, 1215 Jefferson Davis Highway, Suite 1204, Arlington VA 22202-4302. Respondents should be aware that notwithstanding any other provision of law, no person shall be subject to a penalty for failing to comply with a collection of information if it does not display a currently valid OMB control number.</p>				
1. REPORT DATE 14 APR 2005	2. REPORT TYPE N/A	3. DATES COVERED -		
4. TITLE AND SUBTITLE Numerical Analysis of Flow around Rectangular Cylinders with Various Side Ratios			5a. CONTRACT NUMBER	
			5b. GRANT NUMBER	
			5c. PROGRAM ELEMENT NUMBER	
6. AUTHOR(S)			5d. PROJECT NUMBER	
			5e. TASK NUMBER	
			5f. WORK UNIT NUMBER	
7. PERFORMING ORGANIZATION NAME(S) AND ADDRESS(ES) YKK Corp., 200 Yoshida,Kurobe, Toyama, Japan			8. PERFORMING ORGANIZATION REPORT NUMBER	
9. SPONSORING/MONITORING AGENCY NAME(S) AND ADDRESS(ES)			10. SPONSOR/MONITOR'S ACRONYM(S)	
			11. SPONSOR/MONITOR'S REPORT NUMBER(S)	
12. DISTRIBUTION/AVAILABILITY STATEMENT Approved for public release, distribution unlimited				
13. SUPPLEMENTARY NOTES See also ADM001800, Asian Computational Fluid Dynamics Conference (5th) Held in Busan, Korea on October 27-30, 2003. , The original document contains color images.				
14. ABSTRACT				
15. SUBJECT TERMS				
16. SECURITY CLASSIFICATION OF:			17. LIMITATION OF ABSTRACT UU	
a. REPORT unclassified	b. ABSTRACT unclassified	c. THIS PAGE unclassified	18. NUMBER OF PAGES 8	19a. NAME OF RESPONSIBLE PERSON

previous experimental ones. In particular, we have noted the relationship between flow pattern and base pressure coefficient nearby critical depth $D/H=0.6$, compared with the phenomenon in high Reynolds number.

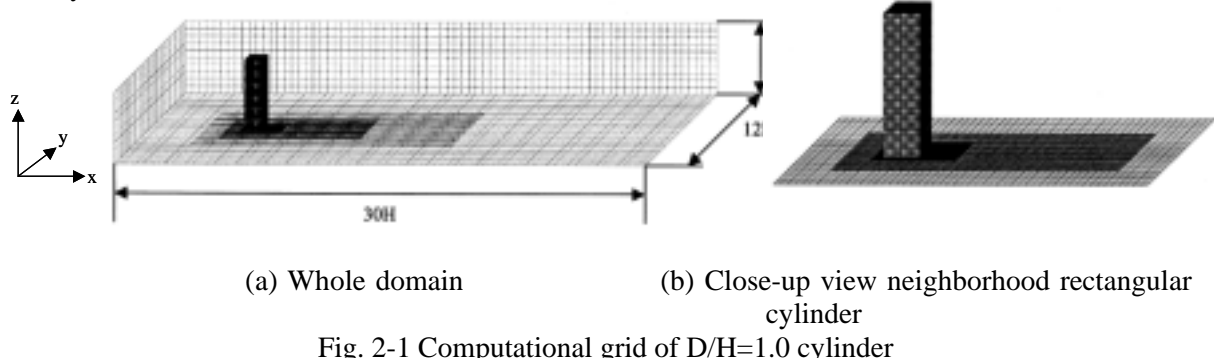
2. Numerical methods

2.1 Governing equations and schemes

A three dimensional continuity equation and Navier-Stokes equation, which is dimensionless by the representative velocity U , where U is the free stream velocity, and the representative length H , where H is the cross-flow direction length of a rectangular cylinder, have been obtained as the governing equations. MAC algorithm has been used for the coupling between pressure and velocity. These governing equations have been approximated by a finite difference scheme. In these equations, the spatial differential terms, except for the convection term of Navier-Stokes equation, have been approximated by a second-order centered scheme, the convection term has been approximated by a third-order upwind scheme⁽⁸⁾. These spatial differential terms have been discretized on regular meshes using a multi directional finite difference scheme⁽⁹⁾ in order to achieve compatibility of high accuracy and robustness. A first-order Euler implicit scheme has been used for time integration. Calculated Reynolds number ($Re = U H / \nu$, ν describes kinematic viscosity of the fluid) is 10^3 .

2.2 Analysis condition

An example of an analysis region is shown in Fig. 2-1. It spreads $6H$ for the upstream region, $24H$ for the downstream region, $6H$ for the side region from the center of a rectangular cylinder and $4H$ for the span wise region. This region is divided into four blocks and these blocks are equally distributed in all spatial directions; the minimum mesh size is $0.05H$ for the block adjacent to the cylinder and $0.2H$ for that in the outer region. Then the multi grid method is used to combine these blocks in order to reduce calculation load by reducing the mesh number. The boundary conditions are as follows; a uniform flow condition is obtained for the inlet region, zero gradient condition for the downstream exit and side boundaries, cyclic condition for the span wise boundary and no-slip condition for the surface of the cylinder.



3. Analysis Results

3.1 Result for $D/H=0.2$ cylinder

The time histories of drag, lift and base pressure coefficients affect to the $D/H=0.2$ cylinder is shown in Fig. 3-1. From temporary variations of drag and base pressure coefficients, it is shown that the mean value of base pressure coefficient increases, that of drag coefficient decreases and the amplitudes of fluctuations of these variables are weak from dimensionless times $t=200$ to 330 . Corresponding to these phenomena, the amplitude of fluctuation of lift coefficient is small. On the other hand, for other times, each fluid force largely fluctuates, the mean value of drag coefficient is large and that of base pressure coefficient is small. The typical flow patterns of these two phenomena are shown in Fig. 3-2 and 3-3. Each flow pattern is shown by vorticity ζ_z distribution, which has a span wise axis, on the center plane of the x - y cross section. When the mean drag coefficient is small and the mean base pressure coefficient is large, the flow separated from the leading edge forms vortex far away from the trailing edge of the cylinder. On the other hand, when the mean drag coefficient is large and the mean base pressure coefficient is small, the flow separated from the leading edge rolls up

in a closer region from the trailing edge. However, in this case, a vortex is formed away from the trailing edge of the cylinder. Because the intensity of the latter vortex is higher than that of the former, it is thought that the pressure fluctuation around the cylinder is larger and the amplitude of fluctuation is larger than former.

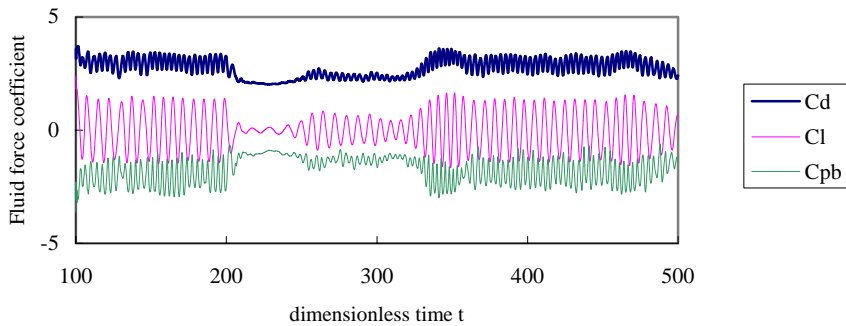


Fig. 3-1 Time history of fluid force of $D/H=0.2$ cylinder

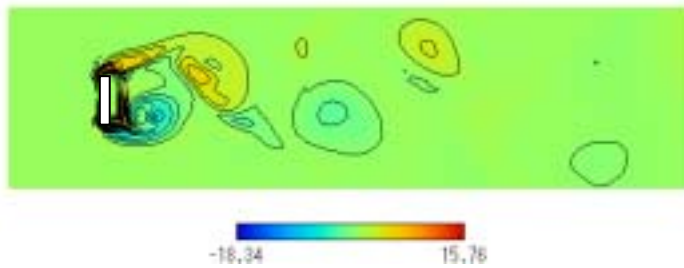


Fig. 3-2 Span wise vorticity component ω_z distribution around $D/H=0.2$ cylinder
(high-pressure mode, $z=2.0H$, $t=300$)

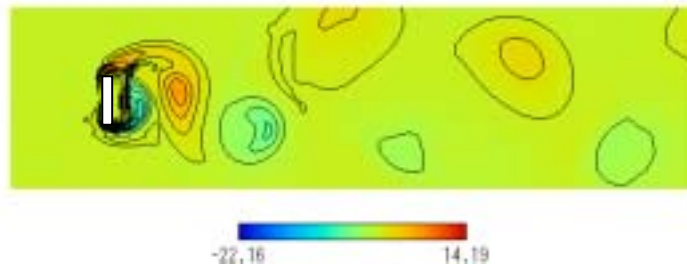


Fig. 3-3 Vorticity distribution around $D/H=0.2$ cylinder (low-pressure mode, $t=388$)

3.2 Result for $D/H=0.4$ cylinder

The time variations of fluid forces affect to the $D/H=0.4$ cylinder, as shown in Fig. 3-4. In this case, in contrast to the case of the $D/H=0.2$ cylinder, it is found that the pattern of large drag with low base pressure and that of small drag with high base pressure alternately appear in a short period. Moreover, the time of low base pressure is longer than that of high base pressure. The flow pattern of this case is shown in Figs. 3-5 and 3-6. In the case of high base pressure (shown in Fig. 3-5), similar to the case of the $D/H=0.2$ cylinder, the flow separated from the leading edge forms a vortex, which is large in the flow direction and diffusive, far away from the trailing edge of the cylinder. On the other hand, it is found that a vortex, which is small in the flow direction and has a high intensity, is formed near the trailing edge of the cylinder by the flow separated from the leading edge in the case of low base pressure. Especially in latter case, being different from the case of the $D/H=0.2$, it is thought that the peak value of base pressure is lower as a result of the vortex formed much closer to the cylinder.

3.3 Result for $D/H=0.6$ cylinder

We show the results for the $D/H=0.6$ cylinder in Figs. 3-7 to 3-9. As shown in Fig. 3-7, the time history of fluid forces is similar to that of the $D/H=0.4$ cylinder and the pattern of large drag with low

base pressure and that of small drag with high base pressure periodically alternate. However in this case, it is confirmed that the time rate holding the state of small drag with high base pressure is increased; therefore the mean drag coefficient takes a small value and the mean base pressure takes a large value. On the other hand, the variation of the flow pattern corresponding to this variation of fluid forces agrees with the case of the $D/H=0.4$ cylinder, as shown in Figs. 3-8 and 3-9.

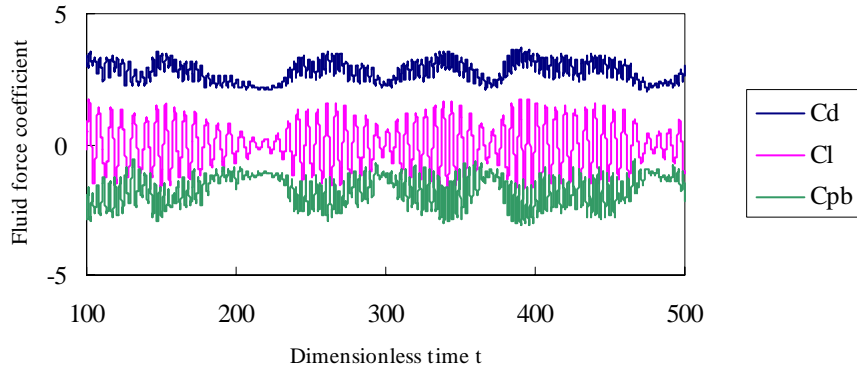


Fig. 3-4 Time history of fluid force of $D/H=0.4$ cylinder

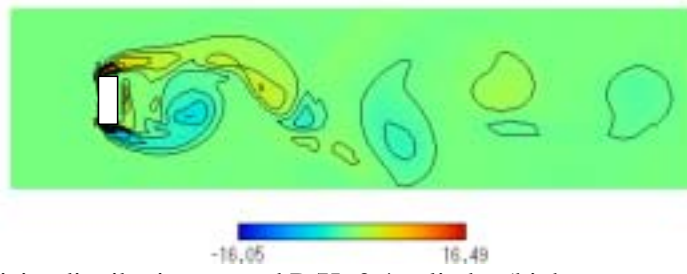


Fig. 3-5 Vorticity distribution around $D/H=0.4$ cylinder (high-pressure mode, $t=226$)

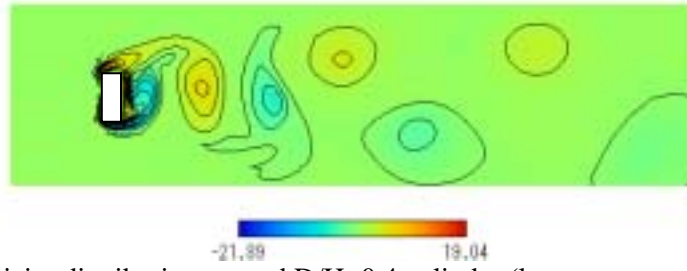


Fig. 3-6 Vorticity distribution around $D/H=0.4$ cylinder (low-pressure mode, $t=342$)

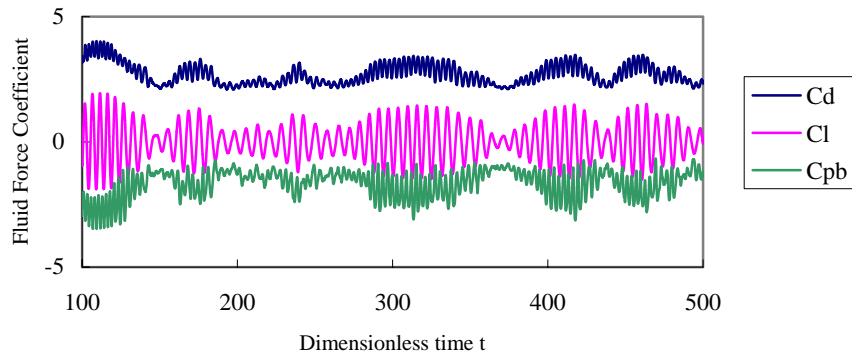


Fig. 3-7 Time history of fluid force of $D/H=0.6$ cylinder

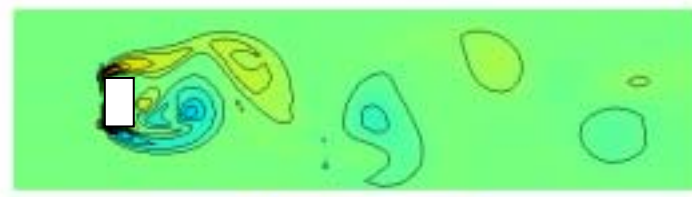


Fig. 3-8 Vorticity distribution around $D/H=0.6$ cylinder (high-pressure mode, $t=377$)

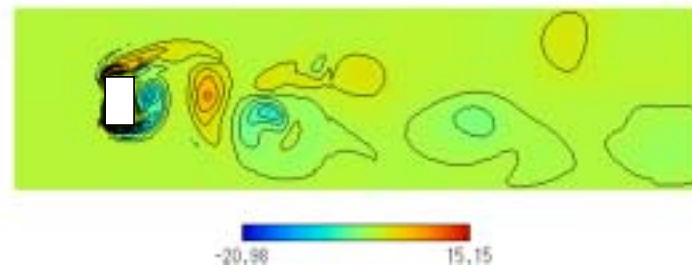


Fig. 3-9 Vorticity distribution around $D/H=0.6$ cylinder (low-pressure mode, $t=326$)

3.4 Result for $D/H=1.0$ cylinder

The result for the $D/h=1.0$ cylinder, which has a square section, is shown in Figs. 3-10 and 3-11. It is found from the effect of the time history of fluid forces of the $D/h=1.0$ cylinder shown in Fig. 3-10 that drag, lift and base pressure coefficients exhibit an almost regular variation different from that in the case of $D/H=0.2-0.6$ cylinders. As shown in Fig. 3-11, the flow pattern of the $D/H=1.0$ cylinder is as follows; the flow separated from leading edge rolls up far away from the trailing edge of the cylinder and the Karman vortices regularly shed from there. It is thought from the time history of fluid forces and the flow pattern that the flow around a $D/H=1.0$ square cylinder corresponds to with large vortices forming of $D/H=0.2-0.6$ cylinders.

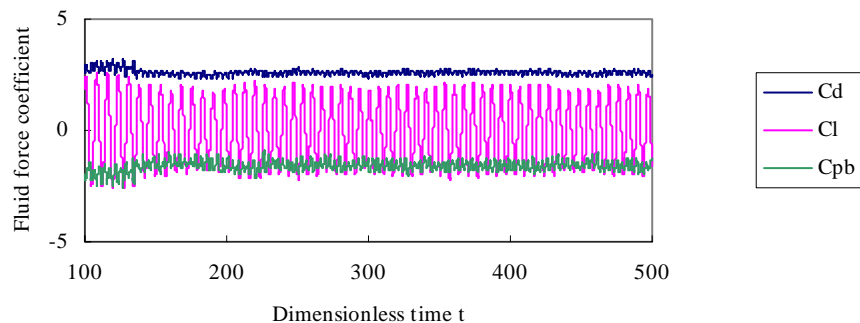


Fig. 3-10 Time history of fluid force of $D/H=1.0$ cylinder

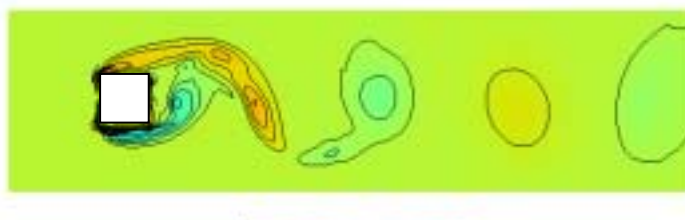
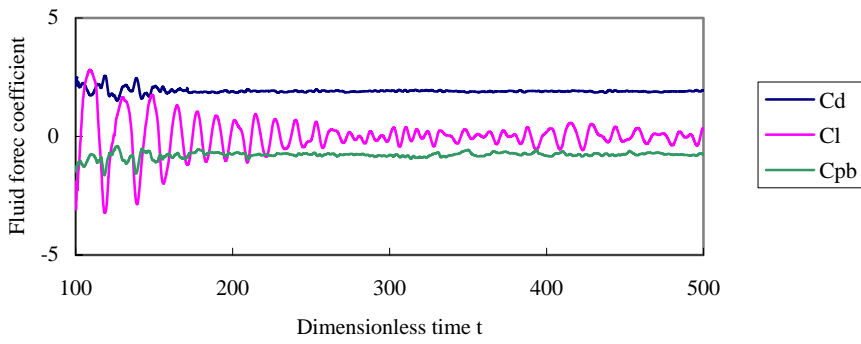
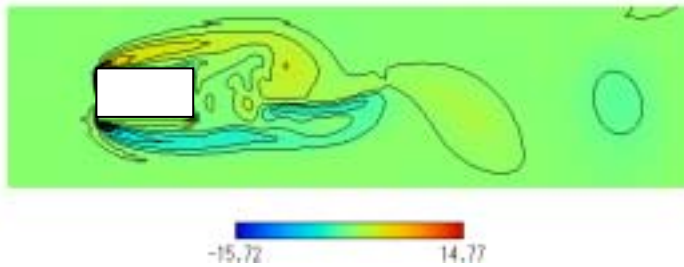
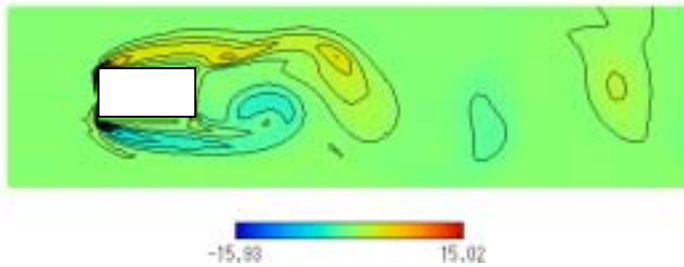


Fig. 3-11 Vorticity component z distribution around $D/H=1.0$ cylinder ($t=371$)

Fig. 3-12 Time history of fluid force of $D/H=2.0$ cylinderFig. 3-13 Vorticity distribution around $D/H=2.0$ cylinder (large fluctuation mode, $t=234$)Fig. 3-14 Vorticity distribution around $D/H=2.0$ cylinder (small fluctuation mode, $t=329$)

3.5 Result for $D/H=2.0$ cylinder

The result for the $D/H=2.0$ cylinder is shown in Figs.3-12 to 3-14. As shown in Fig. 3-12, all effects of fluid forces, drag, lift and base pressure, of the $D/H=2.0$ cylinder are very small and slow. In this case, the flow pattern changes as follows; the flow separated from the leading edge does not reattach to the cylinder side section, rolls up from the trailing edge and forms weak vortices. Therefore, it is thought that the fluctuation of lift coefficient is controlled without forming a separation bubble beside the cylinder and the cycle of vortex shedding is long.

4. Discussions

4.1 Dependence of the variation of fluid forces on side ratios

First, the variation of vortex shedding Strouhal number ($St=fH/U$, f describes the wake vortex shedding frequency) and the mean of base pressure coefficient are shown in Figs. 4-1 and 4-2. The vortex shedding Strouhal number is almost constant value for the $D/H=0.2\text{--}0.6$ cylinders, then decreases as side ratios increase. As observed in Fig. 4-1, the result of this simulation shows good agreement qualitatively and quantitatively with experimental ones obtained by Okajima et al.⁽⁴⁾. On the other hand, since there are two patterns, which have high and low base pressure modes as mentioned above, two values for each pattern are plotted in Fig. 4-2. Concerning this, though the value of the $D/H=0.4$ cylinder is slightly large, it is confirmed that this calculation result qualitatively and

Numerical Analysis of Flow around Rectangular cylinders with Various Side Ratios

quantitatively is in good agreement with experimental data ⁽⁴⁾. Therefore, it is thought that this calculation result simulates fluid dynamic characteristics against the change in side ratio.

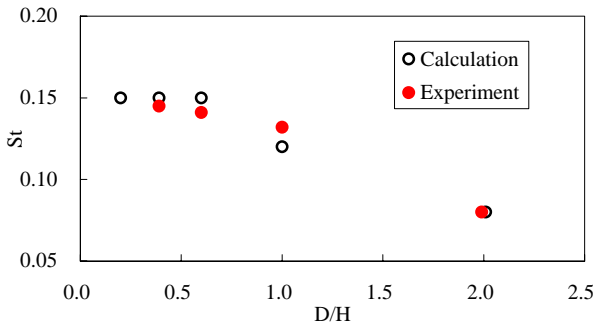


Fig. 4-1 Strouhal number variation with side ratio

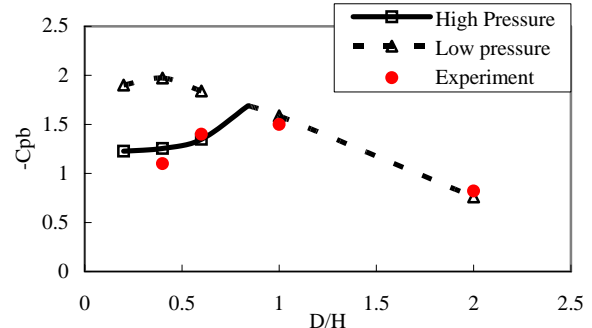


Fig. 4-2 Mean base pressure coefficient variation with side ratio

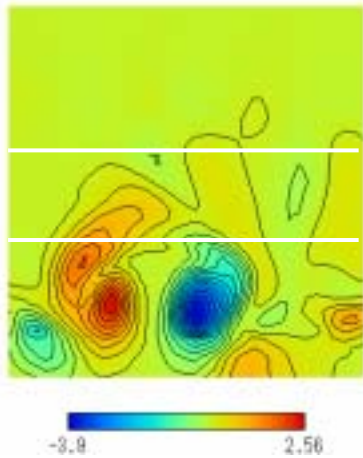


Fig. 4-3 Streamwise vorticity component distribution behind $D/H=0.4$ cylinder
(High pressure mode, $x=3.2H$, $t=226$)

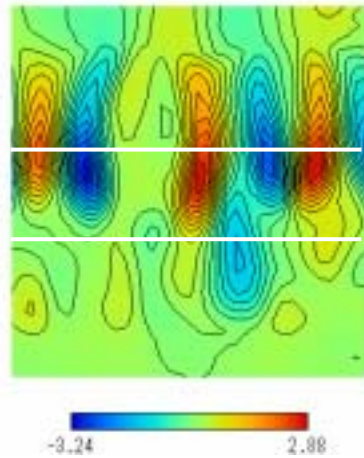


Fig. 4-2 Vorticity distribution behind $D/H=0.4$ cylinder
(Low pressure mode, $t=342$)

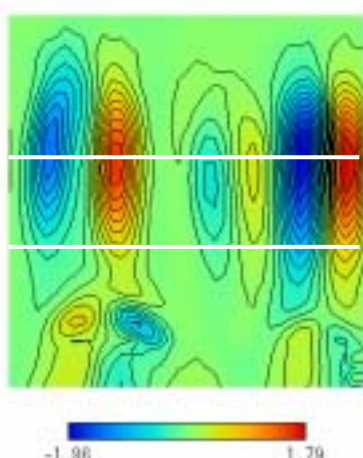


Fig. 4-3 Vorticity distribution behind $D/H=1.0$ cylinder
($x=4.0H$, $t=371$)

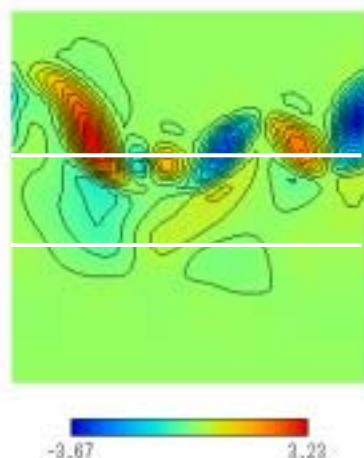


Fig. 4-2 Vorticity distribution behind $D/H=2.0$ cylinder
($x=5.0H$, $t=234$)

4.2 Two characteristic modes; low-pressure and high-pressure modes

It is confirmed by high Reynolds number analysis⁽⁵⁾ that the mode of the large drag coefficient with low base pressure coefficient and that of the small drag coefficient with high base pressure coefficient appears alternately. Thus, we would like to verify the phenomenon in low Reynolds number from this calculation result. Fig. 4-3 shows the vorticity contour of ω_x for the high-pressure mode of the D/H=0.4 cylinder, and Fig.4-4, that for the low-pressure mode of the same cylinder respectively. Moreover, vorticity contour is in the y-z section 3H from the trailing edge of the cylinder. In the high-pressure mode shown in Fig. 4-3, though vortices which have positive and negative values alternately form a line in an almost equal distance of $z=2.0H$, shown corresponding to the vorticity contour of ω_z in Fig. 3-5, vortex forming of ω_z rolls up in the downstream region, and vorticity distribution widely spreads in the span wise direction and is diffusive similar to that of ω_z . On the other hand, in the low-pressure mode shown in Fig. 4-4, similar to the high-pressure mode, though vortices which have positive and negative values stand in a line in equal distance of $z=1.3H$, similar trend to ω_z that is observed the distribution is wide in the height direction and narrow in the span wise direction. Although the peak value of vorticity is nearly equal in the high-pressure and low-pressure modes, vortices which have large distribution and are diffusive are formed in the high-pressure mode and those which have narrow distribution and are condensed are formed in the low-pressure mode. As a result, the effect of the fluid forces of the rectangular cylinders and their fluctuation are large. This variation of the flow pattern is similar to that in high Reynolds number and it is found that fluid dynamic characteristics are affected by the three-dimensional vortex structure of flow in low Reynolds number of $Re=10^3$. Moreover, in the case of the D/H=1.0 cylinder, it is confirmed in Fig. 4-5 that vortices are formed similar to that in the low-pressure mode and as a result, it is thought that fluctuation of lift coefficient is large. In the case of the D/H=2.0 cylinder, it is shown in Fig. 4-6 that vortices have wide distribution in the span wise direction, thus it is thought that fluctuation of fluid force is extremely small.

5. Conclusions

The flow around rectangular cylinders with various side ratios, D/H=0.2-2.0, in Reynolds number $Re=10^3$ was numerically analyzed using multidirectional finite difference and multi grid methods. The following are the result obtained.

The calculation results are compared with experimental results; the propriety of the calculation method used is confirmed since the calculation results agree qualitatively and quantitatively with the experimental results.

It is found for the D/H=0.2-0.6 cylinders that the phenomenon which takes peak values of base pressure and drag is caused by the temporally alternating mode which has low base pressure with large drag and high base pressure with small drag, and it is confirmed that this phenomenon is similar to that in high Reynolds number.

It is found that the effect of magnitude of fluid forces of rectangular cylinders is changed by vortex shedding which forms condensed and strong vortices in the low-pressure mode and diffusive and weak vortices in the high-pressure mode.

References

- [1] Nakaguchi H., Hashimoto K. and Muto S., *J. Jpn. Aero. Soc*, Vol. 16,No. 168,(1968), pp 1-5.
- [2] Bearman P. W. and Trueman D. M., *Aeronautical Quarterly*, 23, (1972), pp 229.
- [3] Ohya Y., *J. Fluids & Structures*, 8 (1994), pp 325.
- [4] Okajima A., Kimura S., Ohtsuyama S. and Ojima A., *J. Struct. Eng. JSCE*, Vol. 44A, (1998), pp 971-977.
- [5] Enya A., Okajima A. and Rokugou A., *Trans. Jpn. Soc. Mech. Eng.*, Vol. 68, No. 670, (2002), pp 1601-1607.
- [6] Hayashi K. and Ohya Y., *Proc. 2001 Meet. Jpn. Soc. Fluid Mech.*, (2001), pp 608-609.
- [7] Hayashi K. and Ohya Y., *Proc. 2002 Meet. Jpn. Soc. Fluid Mech.*, (2002), pp 348-349.
- [8] Kawamura T. and Kuwahara K., *AIAA paper.*, 84-340, (1984).
- [9] Kuwahara K., *AIAA paper.*, 99-3405, (1999).